Sensitivity Analysis of Fluid-Structure Interaction using the PFEM

Minjie Zhu
Post-Doctoral Researcher, School of Civil and Construction Engineering, Oregon State Univ., Corvallis, OR, USA

Michael H. Scott
Associate Professor, School of Civil and Construction Engineering, Oregon State Univ., Corvallis, OR, USA

ABSTRACT: Sensitivity analysis of fluid-structure interaction (FSI) simulations provides an important tool for assessing the reliability and performance of coastal infrastructure subjected to storm and tsunami hazards. As a preliminary step for gradient-based applications in reliability, optimization,system identification, and performance-based engineering of coastal infrastructure, the direct differentiation method (DDM) is applied to FSI simulations using the particle finite element method (PFEM) to compute sensitivities of simulated FSI response with respect to uncertain parameters of the structural and fluid domains that are solved in a monolithic system via the PFEM. Due to geometric nonlinearity of the free-surface flow, geometric sensitivity of the fluid is considered in the governing equations of the DDM along with sensitivity of material nonlinear response in the structural domain. An example application shows sensitivity to load and resistance variables of a reinforced concrete frame subjected to tsunami loading with open and closed first story design configurations.

1. INTRODUCTION

Wave loads induced by tsunami and storm surge events can cause significant damage to critical coastal infrastructure as observed in recent natural disasters such as the 2011 Great East Japan earthquake and tsunami and the Superstorm Sandy hurricane of 2012. The modeling of wave loads as static forces on a deformable body, or conversely, as hydrodynamic forces on a rigid body, may not provide accurate predictions of structural response. To obtain accurate response for structural displacements and forces, fluid-structure interaction must be considered accounting for the kinematics and deformation of both the structural and fluid domains. It is also imperative to assess the sensitivity of structural response to stochastic wave loading and uncertain structural properties. The sensitivity has important implications for the design of coastal infrastructure and in assessing the probability of failure of buildings and bridges in tsunami and storm events as part of an over-arching performance-based engineering framework.

Fluid-structure interaction with incompressible Newtonian fluid is one of the most challenging problems in computational fluid mechanics because the incompressibility condition leads to numerical instability of the computed solution. A large number of Finite Element Methods (FEM) have been developed for the computation of incompressible Navier-Stokes equations using the Eulerian, Lagrangian or Arbitrary Lagrangian-Eulerian (ALE) formulations Girault and Raviart (1986); Gunzburger (1989); Baiges and Codina (2010); Radovitzky and Ortiz (1998); Tezduyar et al. (1992). The particle finite element method (PFEM) Oñate et al. (2004), has been shown to be an effective Lagrangian approach to FSI because it uses the same Lagrangian formulation as structures. A monolithic system of equations is created for the simultaneous solution of the response in the fluid and structural domains via the fractional step method (FSM). This alleviates the need to couple disparate computational fluid and structural modules in order to simulate FSI response, which can lead to unconservative estimates of structural response.

While the PFEM solution of FSI simulations via a monolithic system has computational advantages in determining the fluid and structure response, the sensitivity of this response to uncertain modeling parameters is just as, if not more, important than the response itself. As a standalone product, sensitivity analysis shows the effect of modeling assumptions and uncertain properties on system response, but it also an important component to gradient-based applications. There are two methods for calculating the sensitivity of a simulated response. The finite difference method (FDM) repeats the simulation with a perturbed value for each parameter and does not require additional implementation as perturbations and differencing can be handled with pre- and post-processing. The accuracy of the resulting finite difference approximation depends on the size of the perturbation where the results are not accurate for large perturbations and are prone to numerical round-off error for very small perturbations. Due to the need for repeated simulations, the FDM approach can become inefficient when there is a large number of parameters.

A more accurate approach is the direct differentiation method (DDM), where derivatives of the governing equations are implemented alongside the equations that govern the simulated response. At the one-time expense of derivation and implementation, the DDM calculates the response sensitivity efficiently for each parameter as the simulation proceeds rather than by repeating the analysis. The DDM is generally more accurate than the FDM because the sensitivity is computed using the same numerical algorithm as the response, making it subject to only numerical precision rather than round off. Analytical approaches to sensitivity analysis based on DDM of structural response have been well developed in the literature Kleiber et al. (1997); Scott et al. (2004); Scott and Haukaas (2008), while sensitivity analysis of fluid-structure interaction (FSI) has not been addressed. This is partly due to the complexity of the computation for the FSI response and the cumbersome nature of staggered computational approaches.

2. PFEM Response Computations

This section provides a brief review of the equations that govern FSI response using the PFEM. After applying finite element techniques, discrete algebraic equations are formed from MINI elements in the fluid domain and arbitrary line and solid elements in the structural domain. The algebraic equations will be differentiated in the following section for sensitivity analysis via the DDM.

In the combined equations of fluid and structures, particles connected to both domains are identified as interface particles, whose contributions appear in both fluid and structural equations. Subscripts i, s and f are given to indicate interface, structural and fluid variables and equations

$$\mathbf{M}_{ss}\dot{\mathbf{v}}_s + \mathbf{M}_{si}\dot{\mathbf{v}}_i + \mathbf{C}_{ss}\mathbf{v}_s + \mathbf{C}_{si}\mathbf{v}_i + \mathbf{F}_s^{int}(\mathbf{u}_s, \mathbf{u}_i) = \mathbf{F}_s \tag{1}$$

$$\mathbf{M}_{is}\dot{\mathbf{v}}_s + \left(\mathbf{M}_{ii}^s + \mathbf{M}_{ii}^f\right)\dot{\mathbf{v}}_i + \mathbf{C}_{is}\mathbf{v}_s + \mathbf{C}_{ii}\mathbf{v}_i + \mathbf{F}_i^{int}(\mathbf{u}_s, \mathbf{u}_i) - \mathbf{G}_i\mathbf{p} = \mathbf{F}_i^s + \mathbf{F}_i^f \tag{2}$$

$$\mathbf{M}_{ff}\dot{\mathbf{v}}_f - \mathbf{G}_f\mathbf{p} = \mathbf{F}_f \tag{3}$$

$$\mathbf{G}_f^T\mathbf{v}_f + \mathbf{G}_i^T\mathbf{v}_i + \mathbf{S}\mathbf{p} = \mathbf{F}_p \tag{4}$$

Numerical time integration, such as the backward Euler method, and nonlinear solution algorithm, such as fixed-point iteration, can be applied to the combined equations in order to obtain a monolithic system of equations, which is solved by the fractional step method (FSM).

3. Direct Differentiation of the PFEM

For structural sensitivity analysis, even for nonlinear materials, the configuration is often fixed. However, for large displacement applications such as FSI, additional sensitivity terms that arise from updating the configuration at each iteration must be taken in to account in the derivation of sensitivity equations. The direct differentiation method (DDM) is used here to compute the sensitivity of PFEM analysis with FSM. As in Kleiber et al. (1997), the DDM is applied on the combined FSI Eqs. (1) to (4) to develop the combined FSI sensitivity equations for fluid and structure.

By taking the derivative of the combined FSI Eqs. (1) to (4) with respect to an uncertain parameter θ, the combined sensitivity equations are obtained with assigned subscripts i, s and f

$$\begin{aligned} &\mathbf{M}_{ss}\frac{\partial \dot{\mathbf{v}}_s}{\partial \theta} + \mathbf{M}_{si}\frac{\partial \dot{\mathbf{v}}_i}{\partial \theta} + \mathbf{C}_{ss}\frac{\partial \mathbf{v}_s}{\partial \theta} + \mathbf{C}_{si}\frac{\partial \mathbf{v}_i}{\partial \theta} \\ &+ \mathbf{K}_{ss}\frac{\partial \mathbf{u}_s}{\partial \theta} + \mathbf{K}_{si}\frac{\partial \mathbf{u}_i}{\partial \theta} = \frac{\partial \mathbf{F}_s}{\partial \theta} - \frac{\partial \mathbf{M}_{ss}}{\partial \theta}\dot{\mathbf{v}}_s \\ &- \frac{\partial \mathbf{M}_{si}}{\partial \theta}\dot{\mathbf{v}}_i - \frac{\partial \mathbf{C}_{ss}}{\partial \theta}\mathbf{v}_s - \frac{\partial \mathbf{C}_{si}}{\partial \theta}\mathbf{v}_i - \frac{\partial \mathbf{F}_s^{int}}{\partial \theta} \end{aligned} \tag{5}$$

$$\begin{aligned} &\mathbf{M}_{is}\frac{\partial \dot{\mathbf{v}}_s}{\partial \theta} + (\mathbf{M}_{ii}^s + \mathbf{M}_{ii}^f)\frac{\partial \dot{\mathbf{v}}_i}{\partial \theta} + \mathbf{C}_{is}\frac{\partial \mathbf{v}_s}{\partial \theta} \\ &+ \mathbf{C}_{ii}\frac{\partial \mathbf{v}_i}{\partial \theta} + \mathbf{K}_{is}\frac{\partial \mathbf{u}_s}{\partial \theta} + (\mathbf{K}_{ii} + \mathbf{H}_{ii})\frac{\partial \mathbf{u}_i}{\partial \theta} \\ &+ \mathbf{H}_{if}\frac{\partial \mathbf{u}_f}{\partial \theta} - \mathbf{G}_i\frac{\partial \mathbf{p}}{\partial \theta} = \frac{\partial \mathbf{F}_i^s}{\partial \theta} + \frac{\partial \mathbf{F}_i^f}{\partial \theta} \\ &- \frac{\partial \mathbf{M}_{is}}{\partial \theta}\dot{\mathbf{v}}_s - \left(\frac{\partial \mathbf{M}_{ii}^s}{\partial \theta} + \frac{\partial \mathbf{M}_{ii}^f}{\partial \theta}\right)\dot{\mathbf{v}}_i \\ &- \frac{\partial \mathbf{C}_{is}}{\partial \theta}\mathbf{v}_s - \frac{\partial \mathbf{C}_{ii}}{\partial \theta}\mathbf{v}_i - \frac{\partial \mathbf{F}_i^{int}}{\partial \theta} + \frac{\partial \mathbf{G}_i}{\partial \theta}\mathbf{p} \end{aligned} \tag{6}$$

$$\begin{aligned} &\mathbf{M}_{ff}\frac{\partial \dot{\mathbf{v}}_f}{\partial \theta} - \mathbf{G}_f\frac{\partial \mathbf{p}}{\partial \theta} + \mathbf{H}_{ff}\frac{\partial \mathbf{u}_f}{\partial \theta} + \mathbf{H}_{fi}\frac{\partial \mathbf{u}_i}{\partial \theta} \\ &= \frac{\partial \mathbf{F}_f}{\partial \theta} - \frac{\partial \mathbf{M}_{ff}}{\partial \theta}\dot{\mathbf{v}}_f + \frac{\partial \mathbf{G}_f}{\partial \theta}\mathbf{p} \end{aligned} \tag{7}$$

$$\begin{aligned} &\mathbf{G}_f^T\frac{\partial \mathbf{v}_f}{\partial \theta} + \mathbf{G}_i^T\frac{\partial \mathbf{v}_i}{\partial \theta} + \mathbf{S}\frac{\partial \mathbf{p}}{\partial \theta} + \mathbf{T}_f\frac{\partial \mathbf{u}_f}{\partial \theta} + \mathbf{T}_i\frac{\partial \mathbf{u}_i}{\partial \theta} \\ &= \frac{\partial \mathbf{F}_p}{\partial \theta} - \frac{\partial \mathbf{G}_f^T}{\partial \theta}\mathbf{v}_f - \frac{\partial \mathbf{G}_i^T}{\partial \theta}\mathbf{v}_i - \frac{\partial \mathbf{S}}{\partial \theta}\mathbf{p} \end{aligned} \tag{8}$$

where, the matrices $\mathbf{H}$ and $\mathbf{T}$ account for geometric nonlinear of the fluid response and its influence on the fluid response sensitivity.

4. EXAMPLES

This example is of a tsunami bore impacting a three story reinforced concrete building. The structural model shown in Fig. 1 was developed by Madurapperuma and Wijeyewickrema (2012) for the analysis of water-borne debris and was further analyzed by Zhu and Scott (2014) to demonstrate fluid-structure interaction using the PFEM. To capture material and geometric nonlinearity, each frame member is discretized in to ten displacement-based beam-column finite elements (*dispBeamColumn* in OpenSees) with fiber-discretized cross-sections at the element integration points and the corotational geometric transformation Crisfield (1991). As discussed above, the geometric nonlinear sensitivity of the fluid is considered through geometric tangent stiffness matrices. DDM sensitivity for the frame elements is described in Scott et al. (2004) while that for the corotational transformation is provided in Scott and Filippou (2007).

The cross-section dimensions, reinforcing details, and concrete properties of the frame are shown in Fig. 2. Light transverse reinforcement provides residual concrete compressive strength in the core regions of the members. Zero tensile strength is assumed for the concrete (*Concrete01* in OpenSees) and the longitudinal reinforcing steel is assumed bilinear with elastic modulus 200 GPa, yield strength 420 MPa, and 1% kinematic strain hardening (*Steel01*). Gravity loads and nodal mass were calculated assuming uniform pressure of 4.8 kPa on floor slabs and 1.0 kPa on the roof with tributary width of 6 m.

A refined mesh of beam-column elements is used for the first floor column members in order to represent a design configuration with a closed first floor that resists hydrodynamic loading. A commonly proposed tsunami mitigation strategy is to design buildings with an open first floor configuration that allows fluid to pass through without developing significant impact and drag forces on the structure. This is accomplished by using only one beam-column element for the first floor column members, i.e., a coarse mesh that will not develop a fluid-structure interface.

The tsunami bore has height 4.5 m, initial velocity 2 m/s, and out-of-plane thickness 6 m. The simulation begins at impending impact on the frame. Snap shots of the simulation are shown in Fig. 3 for the case of closed first story with a refined mesh of first floor beam-column elements. The simulation is repeated and shown in Fig. 4 using a single element coarse mesh for an open first story, which allows the fluid passing through the structure.

The roof displacements for the Fig. 3 and Fig. 4 are compared in Fig. 5, where the closed floor has much larger displacement than the open floor. Whereas, in Fig. 6, the axial forces of right col-

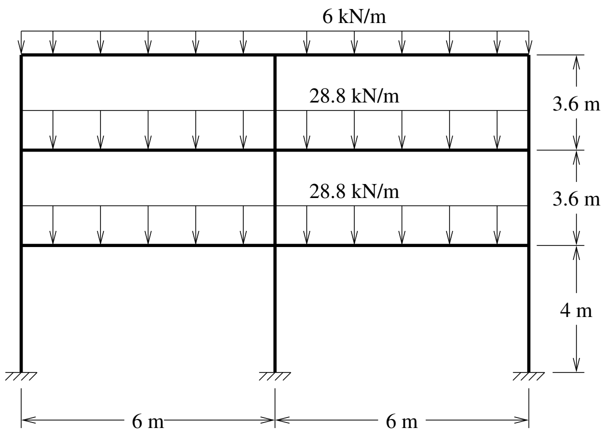

Figure 1: Geometry and floor loads of reinforced concrete frame example.

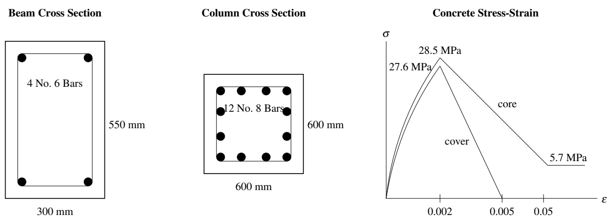

Figure 2: Beam and column cross-sections of reinforced concrete frame.

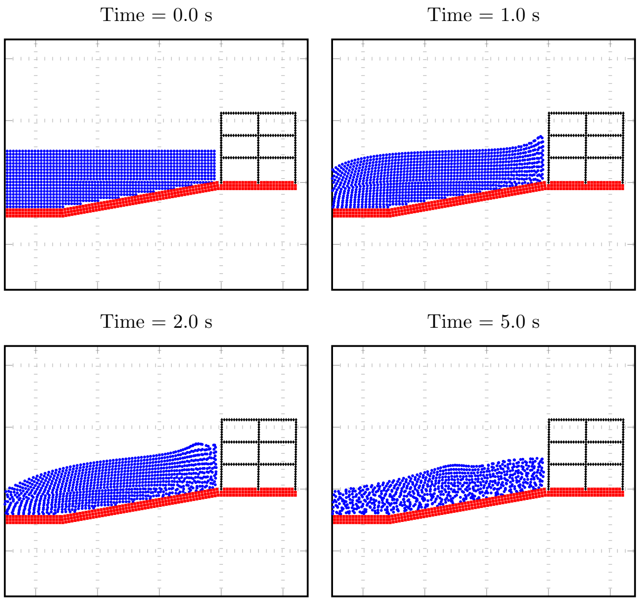

Figure 3: Snap shots of the tsunami waves runup on coastal structure.

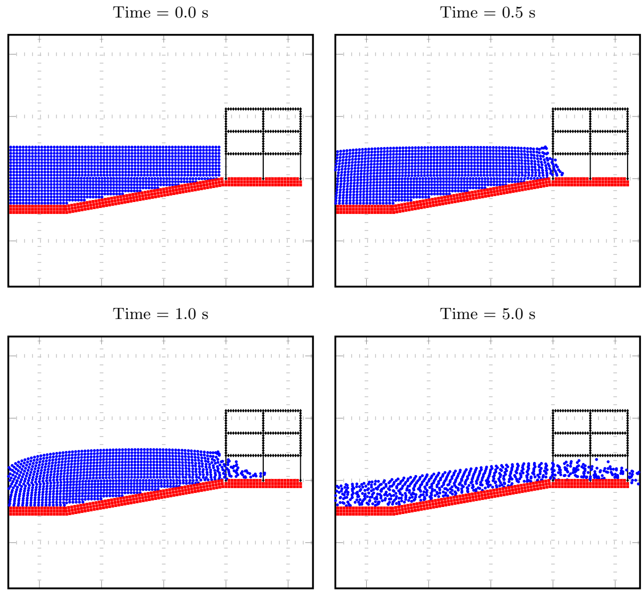

Figure 4: Snap shots of the tsunami waves passing through coastal structure.

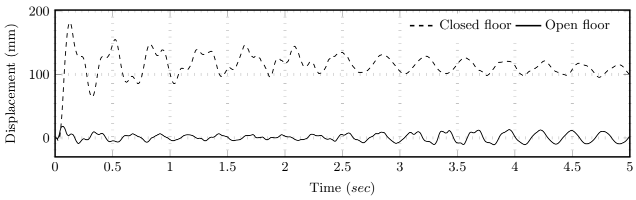

Figure 5: Roof displacements for two cases.

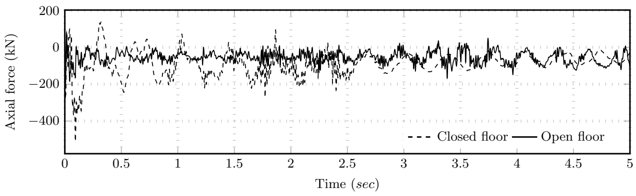

Figure 6: Axial forces at the base of right column for two cases.

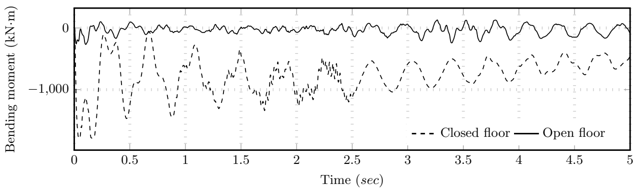

Figure 7: Bending moments at the base of right column for two cases.

umn don't shown much difference between the two cases. This is due to the fact that axial forces of columns are primarily determined by vertical loads rather than the lateral wave loading. The bending moments in Fig. 7, which are greatly influenced by the wave loading, show the difference between two cases.

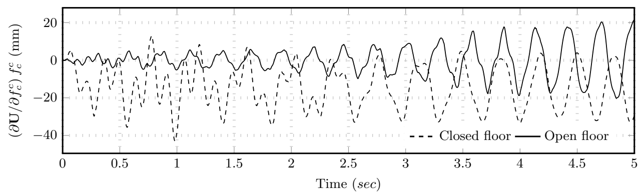

Figure 8: Disp. sens. to f_c^c for two cases.

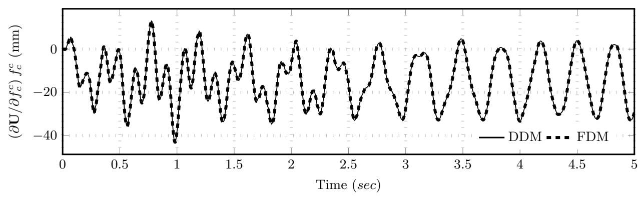

Figure 9: Disp. sens. to f_c^c for closed floor using DDM and FDM.

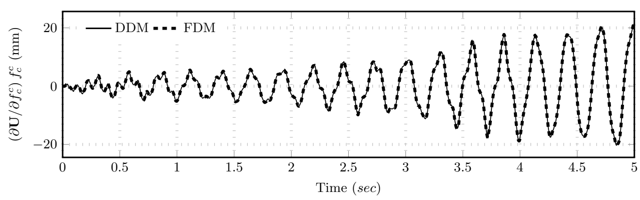

Figure 10: Disp. sens. to f_c^c for open floor using DDM and FDM.

The floor displacement sensitivity to uncertain parameters, the column concrete compressive strength f_c^c and the fluid density ρ_f are shown in Fig. 8 to Fig. 13. The sensitivity to f_c^c are similar for two cases since the similar structures are used. But the sensitivity to ρ_f are very different since the waves are running in different directions.

The bending moment sensitivity to uncertain parameters, the column concrete compressive strength

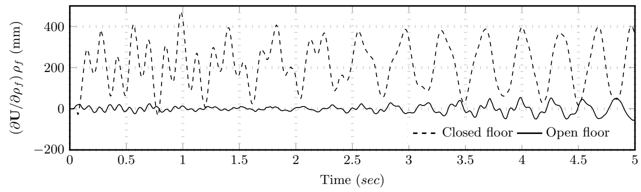

Figure 11: Disp. sens. to ρ_f for two cases.

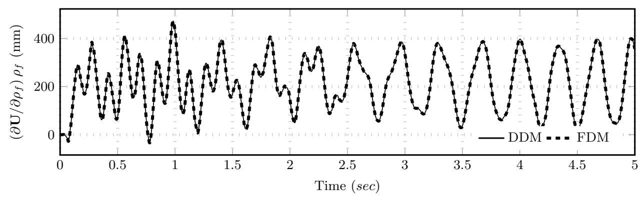

Figure 12: Disp. sens. to ρ_f for closed floor using DDM and FDM.

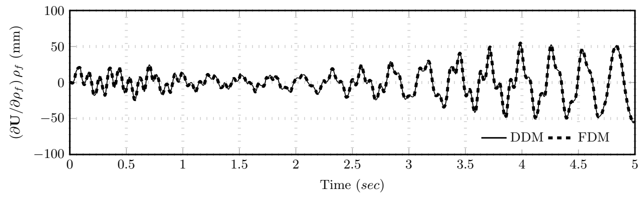

Figure 13: Disp. sens. to ρ_f for open floor using DDM and FDM.

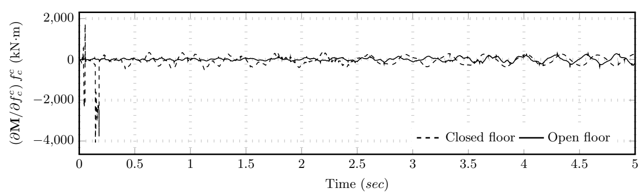

Figure 14: Bending moment sens. to f_c^c for two cases.

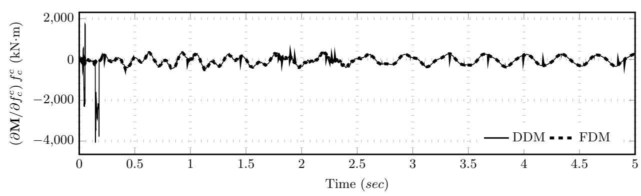

Figure 15: Bending moment sens. to f_c^c for closed floor using DDM and FDM.

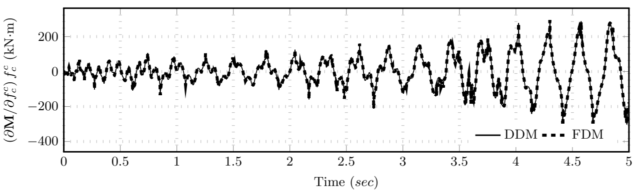

Figure 16: Bending moment sens. to f_c^c for open floor using DDM and FDM.

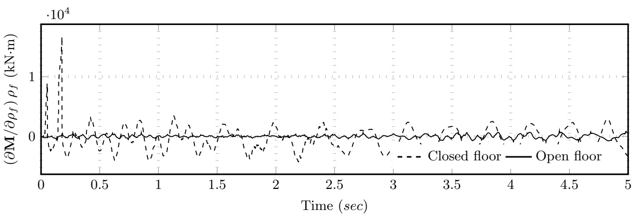

Figure 17: Bending moment sens. to ρ_f for two cases.

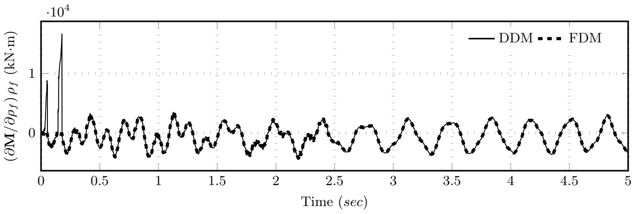

Figure 18: Bending moment sens. to ρ_f for closed floor using DDM and FDM.

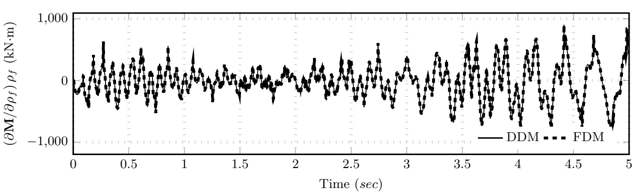

Figure 19: Bending moment sens. to ρ_f for open floor using DDM and FDM.

f_c^c and the fluid density ρ_f are shown in Fig. 14 to Fig. 19.

For all sensitivities, the DDM results are matching to FDM results with a small perturbation between 10^{-8} and 10^{-10}.

5. CONCLUSIONS

The PFEM is an effective approach to simulating FSI because it uses a Lagrangian formulation for the fluid domain, which is the same formulation typically employed for finite element analysis of structures. Development of DDM sensitivity equations for the PFEM broaden its application to gradient-based applications in structural reliability, optimization, and system identification. Due to geometric nonlinearity of the fluid domain, additional terms were required to derive and implement the DDM equations for the PFEM. Following the same analysis procedure as for the response itself, the sensitivity equations are solved using the fractional step method (FSM). Tsunami loading on a reinforced concrete frame verifies the DDM implementation for PFEM with sensitivity results by matching finite difference solutions with small parameter perturbations. Two cases with first floor open and closed are compared in structural responses and sensitivities to various uncertain parameters. Future applications of DDM sensitivity for the PFEM include time variable reliability analysis of fluid-structure interaction, which is an important consideration for multi-hazard analysis involving wind loading concurrent with storm surge and tsunami following an earthquake.

6. ACKNOWLEDGMENTS

This material is based on work supported by the National Science Foundation under Grant No. 0847055. Any opinions, findings, and conclusions or recommendations expressed in this material are those of the authors and do not necessarily reflect the views of the National Science Foundation.

7. REFERENCES

Baiges, J. and Codina, R. (2010). "The fixed-mesh ale approach applied to solid mechanics and fluid-structure interaction problems." *International Journal for Numerical Methods in Engineering*, 81, 1529–1557.

Crisfield, M. A. (1991). *Non-linear Finite Element Analysis of Solids and Structures*, Vol. 1. John Wiley & Sons.

Girault, V. and Raviart, P. (1986). *Finite Element Methods for Navier-Stokes Equations*. Springer-Verlag.

Gunzburger, M. (1989). *Finite Element Methods for Viscous Incompressible Flows*. Academic Press.

Kleiber, M., Antunez, H., Hien, T., and Kowalczyk, P. (1997). *Parameter Sensitivity in Nonlinear Mechanics*. John Wiley & Sons.

Madurapperuma, M. A. K. M. and Wijeyewickrema, A. C. (2012). "Inelastic dynamic analysis of an RC building impacted by a tsunami water-borne shipping container." *Journal of Earthquake and Tsunami*, 6(1), 1250001 1–17.

Oñate, E., Idelsohn, S., Pin, F. D., and Aubry, R. (2004). "The particle finite element method. an overview." *International Journal of Computational Methods*, 1(2), 267–307.

Radovitzky, R. and Ortiz, M. (1998). "Lagrangian finite element analysis of newtonian fluid flows." *International Journal for Numerical Methods in Engineering*, 43, 607–619.

Scott, M. H. and Filippou, F. C. (2007). "Exact response gradients for large displacement nonlinear beam-column elements." *Journal of Structural Engineering*, 133(2), 155–165.

Scott, M. H., Franchin, P., Fenves, G. L., and Filippou, F. C. (2004). "Response sensitivity for nonlinear beam-column elements." *Journal of Structural Engineering*, 130(9), 1281–1288.

Scott, M. H. and Haukaas, T. (2008). "Software framework for parameter updating and finite-element response sensitivity analysis." *Journal of Computing in Civil Engineering*, 22, 281–291.

Tezduyar, T., Mittal, S., Ray, S., and Shih, R. (1992). "Incompressible flow computations with stabilized bilinear and linear equal-order-interpolation velocity-pressure elements." *Computer Methods in Applied Mechanics and Engineering*, 95, 221–242.

Zhu, M. and Scott, M. H. (2014). "Modeling fluid-structure interaction by the Particle Finite Element Method in OpenSees." *Computers & Structures*, 132, 12–21.